

# FINITE ELEMENT LIMIT ANALYSIS OF ACTIVE EARTH PRESSURE IN NONHOMOGENEOUS SOILS

Peyman Hamidi<sup>1</sup>, Tohid Akhlaghi<sup>1</sup>, Masoud Hajjalilou Bonab<sup>1</sup>

<sup>1</sup> Department of Engineering, Faculty of Civil Engineering, University of Tabriz, Iran

## Abstract

HAMIDI PEYMAN, AKHLAGHI TOHID, HAJJALILOU BONAB MASOUD. 2016. Finite Element Limit Analysis of Active Earth Pressure in Nonhomogeneous soils. *Acta Universitatis Agriculturae et Silviculturae Mendelianae Brunensis*, 64(4): 1131–1138.

Limit analysis is a useful method to calculate bearing capacity of footings, earth pressure of retaining walls, stability of slopes and excavations. In recent years, many efforts have been focused on stability problems of geotechnical structures with the limit analysis method. The limit analysis method includes the upper and lower bound theorems. By using the two theorems, the range, in which the true solution falls, can be found.

In this paper upper bound finite element limit analysis is used for calculate active earth force on retaining walls in non-homogeneous soils. Elements with linear strain rates cause to eliminate the necessity of velocity discontinuities between the elements. Nonlinear programming based on second order cone programming (SOCP), which has good conformity with Mohr-Coulomb criterion used in this paper. The sensitivity of active earth force against backfill surcharge ( $q$ ), soil layers cohesion ( $C_i$ ), soil layers unit weight ( $\gamma_i$ ) and friction angle between soil and wall ( $\delta_i$ ) is surveyed.

Keywords: nonhomogeneous soil, upper bound, finite element, optimization, nonlinear programming, retaining wall, limit analysis

## INTRODUCTION

Recently, the upper and lower bound theorems of plasticity are widely used to analyze the stability of geotechnical structures. The stability problems include the bearing capacity of foundations, the active and passive earth pressures on retaining walls, and the factor of safety of slopes. By using the two theorems, the range, in which true solution falls, can be found. This range can be narrowed by finding the highest possible lower bound solution and the lowest possible upper bound solution.

The main difficulty in obtaining strict upper bounds via the finite element method is that the flow rule constraint can only be enforced at a finite number of points, yet it is required to hold throughout the discretized structure. Satisfying this requirement becomes especially difficult in the case of cohesive-frictional materials, where the only obvious solution is to use constant strain elements.

By using linear strain elements which is used in this paper, the difficulty is removed.

In all methods of finite element limit analysis, a key aspect is the efficient solution of the arising optimization problem. Linear programming (LP) has been used for a long time, but the need to replace the (invariably nonlinear) yield function by numerous linear inequality constraints means that the computational cost becomes prohibitive for large problems. During the last twenty years there has been considerable progress in the application of nonlinear programming (NLP), which allows the yield function to be treated in its native form. [1]

Retaining wall has been widely used in civil engineering, traffic engineering, hydraulic engineering and the port engineering. The design of retaining wall was mainly based on the earth pressure which was calculated mainly using the prevailing classical Rankine and Coulomb theory. [5]

There are very few studies about active earth pressure in nonhomogeneous soils, while soil deposits are usually nonhomogeneous in nature, and it is clear that investigations dealing with nonhomogeneous soils are required for accurate analysis and design of retaining walls.

In this paper an effective and accurate method is introduced for analysis and design of retaining walls in nonhomogeneous soils based on upper bound finite element formulation. This is a novel method for calculating strict active earth pressure in nonhomogeneous soils and sensitivity of calculated force is evaluated against backfill surcharge ( $q$ ), soil layers cohesion ( $C_i$ ), soil layers unit weight ( $\gamma_i$ ) and friction angle of layers ( $\phi_i$ ) and between soil and wall ( $\delta_i$ ).

## MATERIALS AND METHODS

### Second-Order Cone Programming

Second-order cone programming (also referred to in the literature as conic quadratic optimization) involves an optimization problem of the form

$$\min \sum_{i=1}^n P_i^T z_i + P_f^T z_f$$

$$s.t. \quad z_i \in C_i \quad \forall_i \in \{1, \dots, N\} \quad (1)$$

$$\sum_{i=1}^n A_i z_i + A_f z_f = g$$

Where  $P_i, z_i \in \mathbb{R}^{d_i}$ ,  $P_f, z_f \in \mathbb{R}^{n_f}$ ,  $A_i \in \mathbb{R}^{m \times d_i}$ ,  $A_f \in \mathbb{R}^{m \times n_f}$ ,  $g \in \mathbb{R}^m$  and the sets  $C_i$  are quadratic cones of the form

$$C = \{z \in \mathbb{R}^d : \|z_{2:d}\| \leq z_1, z_1 \geq 0\} \quad (2)$$

Where  $z_{2:d} = [z_2 \dots z_d]^T$ . For brevity in what follows we will also employ the notation

$$(z_1, z_{2:d}) \in C \quad (3)$$

As shorthand for (2). Variables not participating in a cone constraint are called free variables, and these are denoted  $z_i$  in (1). Nothing that the  $p_i$  are self-dual, the dual problem corresponding to (1) is:

$$\max g^T V$$

$$s.t. \quad t_i \in C_i \quad \forall_i \in \{1, \dots, N\}$$

$$A_i^T V + t_i = p_i \quad \forall_i \in \{1, \dots, N\}$$

$$A_f^T V = p_f \quad (4)$$

Where  $V \in \mathbb{R}^m$  and  $t_i \in \mathbb{R}^{d_i}$ . The optimal point must satisfy the following conditions:

$$z_i \in C_i \quad \forall_i \in \{1, \dots, N\}$$

$$t_i \in C_i \quad \forall_i \in \{1, \dots, N\}$$

$$\sum_{i=1}^N A_i z_i + A_f z_f = g \quad (5)$$

$$A_i^T V + t_i = p_i \quad \forall_i \in \{1, \dots, N\}$$

$$A_f^T V = p_f$$

$$Z_i T_i e_i = 0 \quad \forall_i \in \{1, \dots, N\}$$

Where  $X_i, S_i \in \mathbb{R}^{d_i \times d_i}$  and  $e_i = [1 \ 0 \dots 0]^T \in \mathbb{R}^{d_i}$ . The 'arrowhead' matrices  $Z_i$  and  $T_i$  are given by  $\text{mat}(z_i)$  and  $\text{mat}(t_i)$  respectively, where [2]:

$$\text{mat}(w) = \begin{bmatrix} w_1 & w_{2:d}^T \\ w_{2:d} & w_1 I_{d-1} \end{bmatrix}, w \in \mathbb{R}^d \quad (6)$$

### The Drucker-Prager Criterion

It is convenient to decompose the stresses and strains into their spherical and deviatoric components, employing notation

$$\sigma_m = \frac{1}{N} \sum_{i=1}^N \sigma_{ii}, t_{ij} = \sigma_{ij} - \sigma_m \delta_{ij}$$

$$\theta = \sum_{i=1}^N \varepsilon_{ii}, k_{ij} = \varepsilon_{ij} - \frac{1}{N} \theta \delta_{ij} \quad (7)$$

Where  $N$  is the dimension of the tensors and  $\delta$  is Kronecker's  $\delta$ . The yield criterion of Drucker and Prager [3] can be expressed in the form

$$\sqrt{j_2(t)} + a \sigma_m - k \leq 0 \quad (8)$$

Where  $a$  and  $k$  are non-negative material parameters and

$$j_2(t) = \frac{1}{2} \sum_{i,j} t_{i,j}^2 \quad (9)$$

It can easily be seen that the set of plastically admissible stresses

$$S = \{\sigma : f(\sigma) \leq 0\} \quad (10)$$

is a second-order cone (using the Frobenius norm):

$$\left( k - a \sigma_m \frac{1}{\sqrt{2}} t \right) \in C \quad (11)$$

We define the plastic dissipation function as

$$f_p(\varepsilon) = \sup_{\sigma \in S} \sum_{i,j} \sigma_{i,j} \varepsilon_{i,j} \quad (12)$$

and the set of plastically admissible strains (those satisfying the associated flow rule) as

$$\varepsilon = \{ \varepsilon : f_p(\varepsilon) < +\infty \} \quad (13)$$

The following two cases are considered:

- $a = 0$ . The Drucker-Prager criterion reduces to the von Mises criterion, giving

$$\begin{aligned} f_p(\varepsilon) &= +\infty & \text{if } \theta \neq 0 \\ f_p(\varepsilon) &= 2k\sqrt{j_2(\varepsilon)} & \text{if } \theta = 0 \end{aligned} \quad (14)$$

- $a > 0$ . It is convenient to introduce an auxiliary variable  $\Gamma$  and set  $\theta = a\Gamma$ , leading to

$$\begin{aligned} f_p(\varepsilon) &= +\infty & \text{if } \Gamma < 2\sqrt{j_2(k)} \\ f_p(\varepsilon) &= K\Gamma & \text{if } \Gamma \geq 2\sqrt{j_2(k)} \end{aligned} \quad (15)$$

In these equations  $j_2(k)$ , the second invariant of the deviatoric strain tensor, is defined in the same way as  $j_2(t)$  above. Expressions equivalent to (14) and (15) are given by Salençon, though they can also be obtained directly from the definition (12), using the fact that  $S$  is a self-dual cone. Concerning the dissipation function for plastically admissible strains, it holds that

$$f_p = K\Gamma, \text{ with } \theta = a\Gamma \text{ and } \begin{cases} \Gamma = 2\sqrt{j_2(k)} & \text{if } a=0 \\ \Gamma = 2\sqrt{j_2(k)} & \text{if } a>0 \end{cases} \quad (16)$$

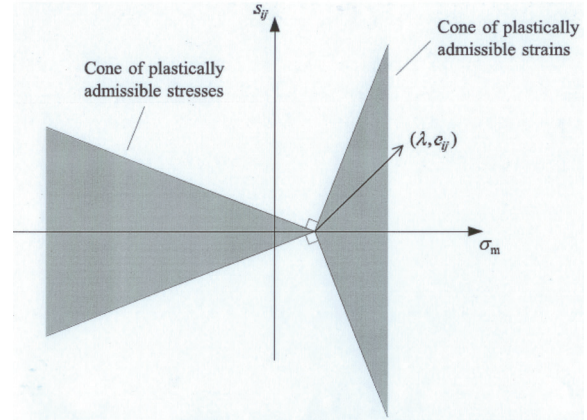
However, since in the application of the kinematic theorem the dissipation will have to be minimized, we can consider that when  $a=0$  the set of the plastically admissible strains is the same as when  $a>0$ , i.e. finally we have

$$f_p = k\Gamma, \text{ with } \theta = a\Gamma \text{ and } \Gamma \geq 2\sqrt{j_2(k)} \quad (17)$$

We notice that, as with the stresses, the set of plastically admissible strains is a second-order cone:

$$(\Gamma, \sqrt{2k}) \in C \quad (18)$$

A geometric interpretation is given in Figure 1.



1: The set of plastically admissible stresses and strains for the Drucker-Prager criterion Simplex Strain Elements

For a 6-node triangular finite element, the displacement field is given by

$$w(x_1, x_2) = a_0 + a_1x_1 + a_2x_2 + a_3x_1x_2 + a_4x_1^2 + a_5x_2^2 \quad (19)$$

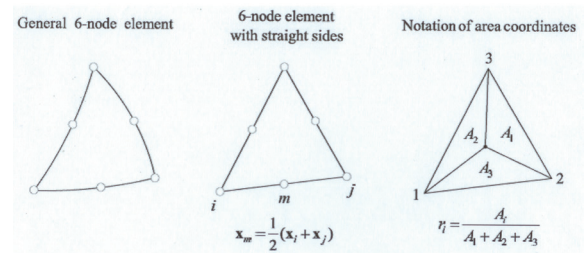
where the vectors  $a_i \in \mathbb{R}^2$  consist of factors depending on the element geometry and the nodal displacements. This means that any strain component varies according to

$$\varepsilon_{kl}(x_1, x_2) = \bar{a}_0 + \bar{a}_1x_1 + \bar{a}_2x_2 \quad (20)$$

and thus the strain tensor at any point within the area of the element can be expressed as a linear combination of those at the three vertices. Moreover, if the sides are straight, the strain tensor at any point in the triangle belongs to the simplex defined by the strain tensors at the vertices, i.e.

$$\varepsilon(x) = \sum_{i=1}^3 h_i(x) \varepsilon_i, \quad 0 \leq h_i(x) \leq 1, \quad \sum_{i=1}^3 h_i(x) = 1 \quad (21)$$

where the coefficients  $ri = hi = Ai / Ael$  are area coordinates with respect to the three vertices. Obviously this also holds for the volume expansion  $\theta$  and the deviatoric strain tensor  $k$  [1].



2: 6-node displacement element for upper bound analysis

### FEM Formulation for Plane Strain and the Mohr-Coulomb Criterion

For plane strain conditions, the Mohr-Coulomb yield criterion has the same form as the Drucker-Prager criterion discussed in Section 3, considering

$$N=2, a=\sin\phi \text{ and } k=c.\cos\phi \quad (22)$$

Where  $c$  is the cohesion and  $\phi$  is the angle of internal friction. Since

$$t_{22}=-t_{11} \text{ and } t_{21}=-t_{12} \quad (23)$$

the yield restriction takes a form similar to (8):

$$\|\mathbf{t}^{red}\| + a\sigma_m - k \leq 0 \quad (24)$$

where  $\mathbf{t}^{red}=[t_{11} \ t_{12}]^T$ . Similarly the dissipation function and flow rule resemble:

$$\dot{f}_p = k\Gamma, \text{ with } \theta = a\Gamma \text{ and } \Gamma \geq \|\mathbf{k}^{red}\| \quad (25)$$

where  $\mathbf{k}^{red}=[2k_{11} \ 2k_{12}]^T$ .

Considering the application of the kinematic theorem to a plane strain structure discretized into NE finite elements, the optimization problem takes the form

$$\begin{aligned} \min \sum_{i=1}^{NE} \int_{(A_i)} k\Gamma dA_i - q_0^T \mathbf{w} \\ \text{s.t. } \Gamma \geq \|\mathbf{k}^{red}\| \text{ in } A_i, \forall i \in \{1, \dots, NE\} \\ \alpha\Gamma = B_m \mathbf{w} \text{ in } A_i, \forall i \in \{1, \dots, NE\} \\ k^{red} = B_d \mathbf{w} \text{ in } A_i, \forall i \in \{1, \dots, NE\} \\ q^T \mathbf{w} = 1 \end{aligned} \quad (26)$$

where  $\mathbf{q}, \mathbf{q}_0$  are vectors of equivalent nodal loads arising from the surface tractions  $\mathbf{l}, \mathbf{l}_0$  and body forces  $\mathbf{b}, \mathbf{b}_0$ . As before, the subscript 0 denotes constant loads that are not subjected to the load multiplier. The matrices  $\mathbf{B}_m$  and  $\mathbf{B}_d$  can easily be derived from the usual strain-displacement relations. For conciseness we have assumed in (26), and in what follows, that  $\mathbf{w} = \mathbf{0}$  on  $S_u$ .

To solve the problem, it is necessary to define flow rule points for each element so that the strain-displacement relations only need to be evaluated at a finite number of points, while also ensuring that the flow rule holds over the whole area of the element. The integral of the dissipation function in (26), considering that  $\Gamma$  varies as a simplex can then be calculated as

$$\int_A k\Gamma dA = \sum_{i=1}^3 \bar{k}_i \Gamma_i \quad (27)$$

where

$$\bar{k}_i = \int_A h_i(\mathbf{x}) k(\mathbf{x}) dA \quad (28)$$

in which  $h_i$  is the relevant area coordinate, see (21) and Figure 2. The value of  $a (= \sin \phi)$  is required to be constant within a given element to ensure that the flow rule is satisfied rigorously. So in terms of the Mohr-Coulomb parameters,  $c$  can vary within an element but  $\phi$  cannot. If both  $c$  and  $\phi$  are constant

then  $\bar{k}_i = k A_{el} / 3$  where  $A_{el}$  is the area of the element. We can now formulate (26) as a standard SOCP problem, cf. (1):

$$\begin{aligned} \min \sum_{i=1}^{NP} \mathbf{c}_i^T \mathbf{x}_i - \mathbf{q}_0^T \mathbf{w} \\ \text{s.t. } \mathbf{x}_i \in C_i \quad \forall i \in \{1, \dots, NP\} \\ A_i \mathbf{x}_i - B_i \mathbf{w} = 0 \quad \forall i \in \{1, \dots, NP\} \\ q^T \mathbf{w} = 1 \end{aligned} \quad (29)$$

where

$$\begin{aligned} \mathbf{c}_i \in \Re^3 \quad \mathbf{c}_i^T &= [\bar{k}_i \ 0 \ 0] \\ \mathbf{x}_i \in \Re^3 \quad \mathbf{x}_i^T &= [\Gamma_i \ (\mathbf{e}_i^{red})^T] \\ \mathbf{A}_i \in \Re^{3 \times 3} \quad \mathbf{A}_i &= \text{diag}[a_i \ 1 \ 1] \\ \mathbf{A}_i \in \Re^{3 \times NU} \quad \mathbf{B}_i &= \begin{bmatrix} \mathbf{B}_{m,i} \\ \mathbf{B}_{d,i} \end{bmatrix} \end{aligned}$$

Here NP is the total number of the flow rule points ( $NP = 3 \times NE$ ) and NU is the total number of degrees of freedom (double the number of nodes, excluding those on  $S_u$ ). The dual problem corresponding to (29) is as follows:

$$\begin{aligned} \max \beta \\ \text{s.t. } (\bar{y}_{m,i} + \bar{y}_{d,i}) \in C_i \quad \forall i \in \{1, \dots, NP\} \\ \begin{cases} \bar{y}_{m,i} + a_i \bar{\sigma}_{d,i} = \bar{k}_i & \forall i \in \{1, \dots, NP\} \\ \bar{y}_{d,i} + \bar{t}_i^{red} = 0 & \forall i \in \{1, \dots, NP\} \end{cases} \\ \sum_{i=1}^{NP} B_{m,i}^T \bar{\sigma}_{m,i} + \sum_{i=1}^{NP} B_{d,i}^T \bar{t}_i^{red} - \beta \mathbf{q} = \mathbf{q}_0 \end{aligned} \quad (30)$$

Expressing now the variables

$\bar{y}_{m,i}$  and  $\bar{\sigma}_{d,i}$  and  $\bar{t}_i^{red}$  in terms of  $\eta_i = A_{el,i} / 3$  (where  $A_{el,i}$  is the area of the element to which the  $i$ th flow rule point belongs) we obtain after some additional manipulations [1]:

$$\begin{aligned}
& \max \beta \\
& s.t. (y_{m,i} t_i^{red}) \in C_i \quad \forall i \in \{1, \dots, NP\} \\
& y_{m,i} + a_i \sigma_{m,i} = k_i^* \quad \forall i \in \{1, \dots, NP\} \\
& \sum_{i=1}^{NP} G_{m,i} \bar{\sigma}_{m,i} + \sum_{i=1}^{NP} G_{d,i} t_i^{red} - \beta q = q_0
\end{aligned} \quad (31)$$

Where  $G_{m,i} = \eta_i B_{m,i}^T$ ,  $G_{d,i} = \eta_i B_{d,i}^T$  and  $k_i^* = \bar{k}_i / \eta_i$  ( $= k_i$  for constant  $k$ ). Note that when  $a > 0$ , the variables  $\sigma_{m,i}$  can easily be eliminated (along with the equalities  $y_{m,i} + a_i \sigma_{m,i} = k_i^*$ ) as described in [4].

### Active earth pressure on retaining walls

Retaining walls has been widely used in civil engineering, traffic engineering, hydraulic engineering and the port engineering. The design of retaining walls was mainly based on the earth pressure which was calculated mainly using the prevailing classical Rankine and Coulumb theory. It was proven that the calculation result of passive earth pressure is larger than the actual situation, and also each of them have certain application conditions (Peng, 2008). Rankine's theory can be used when the wall back-surface is smooth and vertical, also the backfill surface should be horizontal, while the Coulumb's earth pressure theory can be used when the backfill is cohesionless soil. But it is difficult to meet these conditions in practical project. In view of the shortage of prevailing classical theory to calculate earth pressure, it had been extensively studied by scholars at home and abroad. Mazindrani *et al.* (1997), Gnanapragasam (2000) analyzed the earth pressure acting on retaining wall with inclined backfill surface and cohesive soil. Zheng *et al.* (2006) considered the cohesion of clay as a single calculation factor, and the corresponding formula was derived by using limit analysis method for calculate the active earth pressure of the clay subgrade retaining wall. Nian *et al.* (2002) developed a theoretical solution of active and passive earth pressure of cohesive backfill with

inclined surface under surcharge on the basis of lower-bound theorem of limit analysis. Lu (2002) proposed a formula of active earth pressure on retaining wall which considers the cohesion force on sliding plane and the adhesive force on interface of soil and retaining wall. Yang *et al.* (2011) derived a unified solution for the distribution, total force, location of the resultant, active and passive earth pressures on retaining wall and the reacting force on failure surface using differential slice method and graphic method based on the plane failure surface hypothesis and the limit equilibrium theory, and the solution was applied to the case with a battered wall, inclined ground surface, cohesive backfill and distributed surcharge on the ground surface. Hu (2006) improved the Coulumb accurate solution of active earth pressure to cohesive soil which considered the cohesion force on slip surface and adhesive force on interface of retaining wall based on sliding plane hypothesis of Coulumb earth pressure theory. Lin *et al.* (2008) deduced the analytical solution of active earth pressure acting on retaining wall by using the thin layer element method under complicated circumstances. Xu *et al.* (2002), Duncan *et al.* (2001) studied the passive earth pressure by model tests, and some good conclusions were achieved. [5]

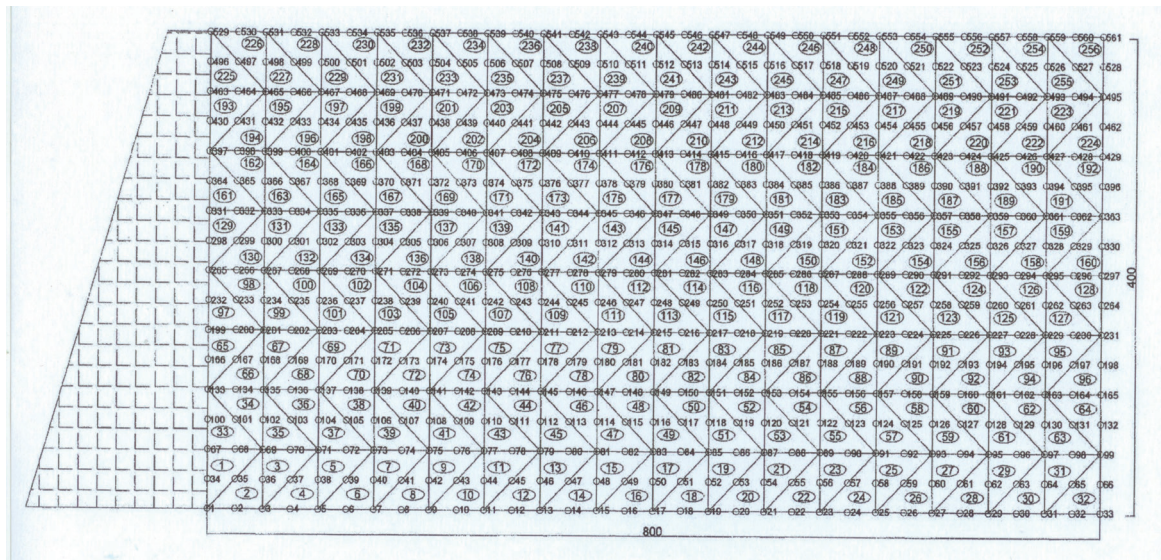
Homogeneous soil has been investigated in previous studies. Although natural soil deposits are dominantly nonhomogeneous, few studies have been conducted on active earth pressure in nonhomogeneous soils. Consequently, further studies dealing with nonhomogeneous soils are required for conducting an accurate analysis and designing the retaining walls.

In this paper, an effective and accurate method is proposed for analyzing and designing the retaining walls in nonhomogeneous soils based on the above-mentioned upper bound finite element formulation. This is a new method for calculating the strict active earth pressure in nonhomogeneous soils in which sensitivity of the calculated force against the backfill surcharge( $q$ ), cohesion of the soil layers ( $C_i$ ), unit

I: Active earth force on retaining wall in homogenous soil (kN/m)

$\alpha$ (deg.)	$H$ (m)	$\beta$ (deg.)	$\gamma$ (kN/m <sup>3</sup> )	$q$ (kN/m <sup>2</sup> )	$C$ (kN/m <sup>2</sup> )	$\phi$ (deg.)	$\delta$ (deg.)	Coulomb method	Proposed upper bound method	Error (%)
90°	4	0	18	10	0	20	0	90.21	90.21	0
90°	4	0	19	10	0	20	5	89.25	89.40	0.17
90°	4	0	20	10	0	20	10	89.35	89.97	0.69
90°	4	0	18	10	0	20	15	79.93	81.22	1.61
90°	4	0	19	10	0	30	0	64	64	0
90°	4	0	20	10	0	30	10	61.7	61.89	0.31
90°	4	0	18	10	0	30	15	55.46	55.87	0.74
90°	4	0	19	10	0	30	20	57.08	57.85	1.35





3: 6-node displacement element for upper bound analysis

weight of the soil layers ( $\gamma_i$ ) and friction angle of the layers ( $\phi_i$ ) and friction angle between the soil and the wall ( $\delta$ ) are measured.

Two-dimensional problems of the plane strain, herein exemplified, follow the Mohr-Coulomb criterion. The program has been written in MATLAB, which creates the geometry, formulates optimization, and solves the problem. The interior-point algorithm is used for solving the optimization problem and fmincon solver from the MATLAB optimization toolbox is used, too. In order to verify the method, at first, a benchmark problem is solved and the results are compared using the well-known methods, then the main problem will be solved.

#### Active Earth Pressure on Retaining Walls in Homogeneous Soils

In order to verify the program, active earth pressure on the retaining wall in homogeneous soil is calculated both using the limit equilibrium method-based coulomb theory and the proposed upper bound method and the results are compared.

For upper bound analysis, a mesh of triangles, as shown in figure 3, composed of 256 triangular six-node elements were compared using the coulomb limit equilibrium method and the results were summarized in Table I. If there is not any surcharge on the backfill, the boundary condition for dual problem and for the nodes on the surface of the backfill ( $N = 529 - 561$ ) is  $\delta_{11} = \delta_{22} = \delta_{12} = 0$ . Clearly, the results of the proposed upper bound are very close to those obtained for homogeneous soil using the coulomb method.

#### Active Earth Pressure on Retaining Wall in Nonhomogeneous Soils

Calculating the active earth pressure on the retaining walls in nonhomogeneous soils is one of the controversial problems in area of the applied soil mechanics. Proposed upper bound method provides a new solution for calculating the active earth force in this condition. For evaluating the effect of each parameter on the resultant active force on the retaining wall, all parameters are changed and the results are shown in figures 4-7. All physical, mechanical, and geometrical parameters are as follow:

$H_1$ : thickness of top layer of soil

$H_2$ : thickness of bottom layer of soil

$\beta$ : wall inclination angle

$\alpha$ : backfill surface angle

$q$ : backfill surcharge

$C_1$ : cohesion of top layer of soil

$C_2$ : cohesion of bottom layer of soil

$\phi_1$ : friction angle of top layer of soil

$\phi_2$ : friction angle of bottom layer of soil

$\delta_1$ : friction angle between top layer of soil and wall

$\delta_2$ : friction angle between bottom layer of soil and wall

$\gamma_1$ : unit weight of top layer of soil

$\gamma_2$ : unit weight of bottom layer of soil

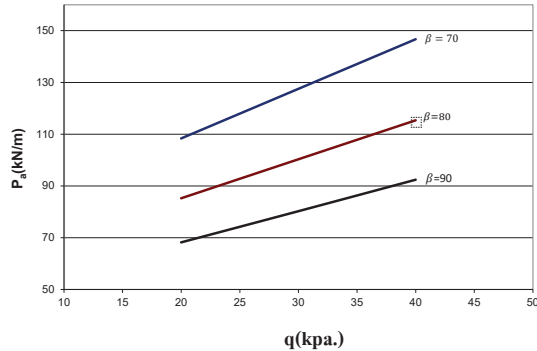
#### Effect of Wall Inclination ( $\beta$ ) and Backfill Surcharge ( $q$ ) on Active Earth Force:

Effect of wall inclination ( $\beta$ ) and backfill surcharge ( $q$ ) on active earth force is shown in figure (4). In this figure other parameters are:

$$C_1 = C_2 = 0, \alpha = 0, \delta = 2\phi/3, \phi_1 = \phi_2 = 30^\circ,$$

$$H_1 = 2m, H_2 = 2m, \gamma_1 = 18 \text{ KN/m}^3, \gamma_2 = 19 \text{ KN/m}^3$$

It is clear that both the wall inclination ( $\beta$ ) and backfill surcharge ( $q$ ) have a significant effect on active earth force, wherein the force is increased by increasing  $q$  and decreasing  $\beta$  as shown in figure (4).



4: Effect of wall inclination ( $\beta$ ) and backfill surcharge ( $q$ ) on  $P_a$ -values

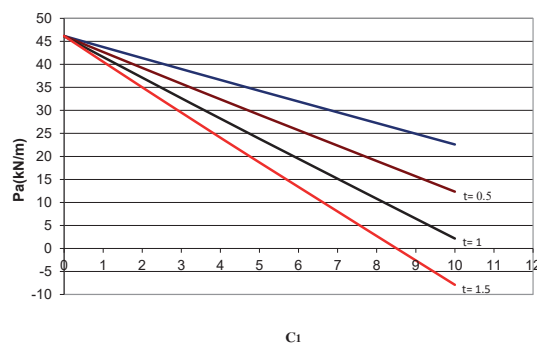
#### Effect of Top Layer Cohesion ( $C_1$ ) and Cohesion Ratio ( $t = C_2/C_1$ ) on Active Earth Force:

Effect of top layer cohesion ( $C_1$ ) and cohesion ratio ( $t = C_2/C_1$ ) is shown in figure (5).

In this figure other parameters are:

$$\alpha = 0, \delta = 2\phi/3, \phi_1 = 25^\circ, \phi_2 = 30^\circ, H_1 = 2m, q = 0, H_2 = 2m, \gamma_1 = 18 \text{ KN/m}^3, \gamma_2 = 19 \text{ KN/m}^3, \beta = 90^\circ$$

It is clear that both the top layer cohesion ( $C_1$ ) and cohesion ratio ( $t = C_2/C_1$ ) are effective parameters on active earth force, wherein the force is decreased by increasing ( $C_1$ ) and ( $t$ ).



5: Effect of Top Layer Cohesion ( $C_1$ ) and Cohesion Ratio ( $t = C_2/C_1$ ) on  $P_a$ -values

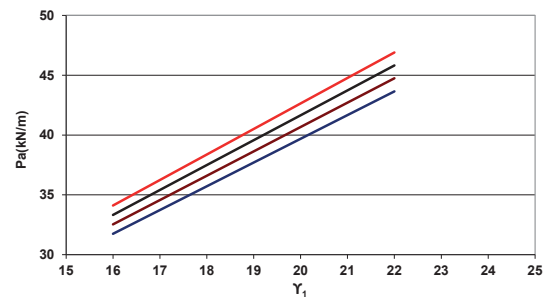
#### Effect of Top Layer Unit Weight ( $\gamma_1$ ) and Unit Weight Ratio ( $r = \frac{\gamma_2}{\gamma_1}$ ) on Active Earth Force:

Effect of top layer unit weight ( $\gamma_1$ ) and unit weight ratio ( $r = \frac{\gamma_2}{\gamma_1}$ ) on active earth force is shown in figure (6).

In this figure other parameters are:

$$H_1 = 2m, H_2 = 2m, \alpha = 0, q = 0, C_1 = 0, C_2 = 0, \phi_1 = 30^\circ, \phi_2 = 35^\circ, \delta = 2\phi/3, \beta = 90^\circ$$

It is clear that these two parameters have a significant effect on active earth force acting on retaining wall in nonhomogeneous soils, wherein



6: Effect of top layer unit weight ( $\gamma_1$ ) and unit weight ratio ( $r = \gamma_2/\gamma_1$ ) on  $P_a$ -values

increasing in both parameters cause an increase in the force.

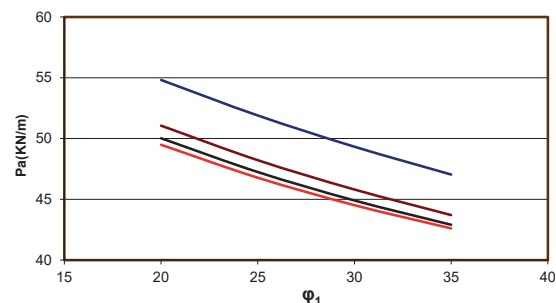
#### Effect of Top Layer Friction Angle ( $\phi_1$ ) and Interface Friction Angle Ratio ( $k = \delta/\phi$ ) on Active Earth Force:

Effect of top layer friction angle ( $\phi_1$ ) and interface friction angle ratio on active earth force is shown in figure (7).

In this figure other parameters are:

$$H_1 = 2m, H_2 = 2m, \alpha = 0, q = 0, C_1 = 0, C_2 = 0, \phi_2 = 30^\circ, \beta = 90^\circ, \gamma_1 = 18 \text{ KN/m}^3, \gamma_2 = 20 \text{ KN/m}^3$$

According to figure (7) top layer friction angle has an important role in active earth force acting on retaining wall in nonhomogeneous soil, while increasing in ( $S$ ) from zero to 0.33 has a significant effect in  $P_a$  and further increase in ( $S$ ) has insensible effect on  $P_a$ . However,  $P_a$  is increased by increasing  $\phi$  and decreasing  $S$ .



7: Effect of top layer friction angle ( $\phi_1$ ) and interface friction angle ratio ( $S = \delta/\phi$ ) on  $P_a$ -values

## DISCUSSION AND CONCLUSION

As shown in figures 4–7, the results are summarized as follow:

1. Active earth force on retaining wall is increased by increasing backfill surcharge ( $q$ ).
2. Increasing the wall inclination ( $\beta$ ) decreases active earth force on the wall.
3. Active earth force on retaining wall is decreased by increasing the top layer cohesion ( $C_1$ ).
4. Cohesion ratio ( $t = C_2 / C_1$ ) is an important parameter on active earth force which increase in ( $t$ ) afford decreasing active earth force on retaining wall.
5. Increasing the top layer unit weight ( $\gamma_1$ ) increases active earth force on the wall.
6. Active earth force on retaining wall is increased by increasing the unit weight ratio ( $r = \gamma_2 / \gamma_1$ ).
7. Top layer friction angle ( $\phi_1$ ) is another significant parameter on active earth force which increase in ( $\phi_1$ ) afford increasing active earth force on retaining wall.
8. Increasing the interface friction angle ratio ( $S$ ) decreases active earth force on the wall.

In this paper formulation of upper bound finite element was introduced. Elimination necessity of velocity discontinuities between the elements is an advantage of linear strain elements used in formulation. This is very important, because the accuracy of solution is completely dependent on the position of velocity discontinuities in problems with discontinuities and inappropriate mesh will reduce the accuracy of method. Using second order cone programming (SOCP), which has good conformity with cone yield functions like Mohr-Coloumb, is another important advantage which removes problems of using linear programming algorithms for yield functions such as divergent in the apexes.

Natural soil deposits are dominantly nonhomogeneous, and it is clear that further studies dealing with nonhomogeneous soils are required for conducting an accurate analysis and designing the retaining walls.

In this paper, an effective and accurate method is proposed for analyzing and designing the retaining walls in nonhomogeneous soils based on the above-mentioned upper bound finite element formulation. This is a new method for calculating the strict active earth pressure in nonhomogeneous soils. The results obtained from examples demonstrate that the proposed method is highly effective and precise for analyzing the earth pressure in nonhomogeneous soils.

According to results of analysis, active earth force in nonhomogeneous soils decreases by increasing in wall inclination ( $\beta$ ), the top layer cohesion ( $C_1$ ), Cohesion ratio ( $t = C_2 / C_1$ ) and interface friction angle ratio ( $S$ ), whereas increases by increasing in backfill surcharge ( $q$ ), top layer unit weight ( $\gamma_1$ ), unit weight ratio ( $r = \gamma_2 / \gamma_1$ ) and top layer friction angle ( $\phi_1$ ).

## REFERENCES

- ANDERSEN ED, ROOS C, TERLAKY, T. 2002. Notes on duality in second order and p-order cone optimization. *Optimization*, (51):627–643.
- BINESH S. M, RAEI S. 2014. Upper bound limit analysis of cohesive soils using mesh-free method. *Geomechanics and Geoengineering*, 9(4): 265–278.
- DRUCKER, D. C, PRAGER, W. 1952. Soil mechanics and plastic analysis or limit design. *Quarterly of Applied Mathematics*, 10:157–165.
- LYAMIN, A. V, SLOAN, S. W. 2002. Upper bound analysis using linear finite elements and non-linear programming. *International Journal for Numerical and Analytical Methods in Geomechanics*, 26:181–216.
- MAKRODIMOPOULOS, A., MARTIN, C. M. 2005. *Lower bound limit analysis of cohesive-frictional materials using second-order cone programming*. Technical Report No.OUEL 2278/05. University of Oxford.
- MAKRODIMOPOULOS, A, MARTIN, C. M. 2005. *Upper bound limit analysis using simplex strain elements and second-order cone programming*. Technical Report No.OUEL 2288/05. University of Oxford.
- PASTOR, J., LOUTE, E., THAI, T. H. 2002. Limit analysis and new methods of optimization. In: *Proceedings of the 5th European Conference on Numerical Methods in Engineering*. Paris, 211–219.
- LIU, X. R., OU, M. X., YANG, X. 2013. Upper bound limit analysis of passive earth pressure of cohesive backfill on retaining wall, *Applied Mechanics and Materials*: 895–900.

Contact information

Peyman Hamidi: e-mail:p.hamidi@iaurmia.ac.ir.